Energetic-Electron-Driven Instability in the Helically Symmetric Experiment

C. B. Deng,[1] D. L. Brower,[1] B. N. Breizman,[2] D. A. Spong,[3] A. F. Almagri,[4] D. T. Anderson,[4] F. S. B. Anderson,[4]
W. X. Ding,[1] W. Guttenfelder,[4] K. M. Likin,[4] and J. N. Talmadge[4]

[1]*Department of Physics and Astronomy, University of California, Los Angeles, Los Angeles, California 90095, USA*
[2]*Institute for Fusion Studies, University of Texas, Austin, Texas 78712, USA*
[3]*Oak Ridge National Laboratory, Oak Ridge, Tennessee 37831, USA*
[4]*Department of Electrical and Computer Engineering, University of Wisconsin, Madison, Wisconsin 53706, USA*
(Received 18 February 2009; published 10 July 2009)

Energetic electrons generated by electron cyclotron resonance heating are observed to drive instabilities in the quasihelically symmetric stellarator device. The coherent, global fluctuations peak in the plasma core and are measured in the frequency range of 20–120 kHz. Mode propagation is in the diamagnetic drift direction of the driving species. When quasihelical symmetry is broken, the mode is no longer observed. Experimental observations indicate that the unstable mode is acoustic rather than Alfvénic.

Instabilities driven by energetic ions have been observed in many experiments on tokamaks [1–5] as well as stellarators [6–8]. In general, the resonance condition for passing particles requires velocity of order or greater than the wave phase velocity. Modes can be driven unstable through an inverse Landau damping process when the diamagnetic drift frequency of the driving energetic particle species, ω_s^* ($= k_\theta \frac{T_s}{q_s B L_{ns}}$), is greater than the mode frequency, where k_θ is the poloidal wave number, and L_{ns}, q_s, and T_s are the density scale length, charge, and temperature of the energetic particle species, respectively [9]. Trapped energetic particles with a precessional drift frequency [10,11] matching the mode frequency can also excite instability. The pressure gradient of the resonant particles is the source of free energy which destabilizes the mode. Similar to fast ions, fast electrons can also provide free energy to drive plasma instabilities.

The helically symmetric experiment (HSX) is the first of a new generation of stellarators that exploit the concept of quasisymmetric magnetic fields with a helical direction of symmetry in magnetic field strength [12,13]. In this Letter, we present experimental evidence for a fast-electron-driven instability associated with electron cyclotron resonance heating (ECRH). For HSX, the instability is strongest when energetic electrons are present and well confined, as is the case for quasihelically symmetric (QHS) plasmas with second-harmonic X-mode ECRH. When quasihelical symmetry is broken by increasing the nonsymmetric magnetic ripple, allowing HSX to operate more like a conventional nonsymmetric stellarator, the instability is no longer observed.

Herein, we report on several features of the unstable modes. Observed fluctuations are global, coherent modes that are directly measured in the plasma core and edge with helical structure exhibiting an odd poloidal mode number (m) and toroidal mode number $n = 1$. Fluctuations are present in the frequency range of 20–120 kHz and propagate in the electron diamagnetic drift direction in the

laboratory frame of reference. Mode frequency is weakly dependent on $\imath$ (where $\imath = 1/q$ is the inverse safety factor) indicating a shear Alfvén wave is not the dominant part of the excited spectrum. These results suggest the unstable mode is acoustic.

All data shown are for HSX plasmas with average major radius $\langle R \rangle = 1.2$ m, average minor radius $\langle a \rangle \le 0.15$ m (4 field periods), and magnetic field $B = 0.5$ T. Central-line-averaged electron densities vary over the range 0.2×10^{12} cm^{-3} $\le \bar{n}_e \le 2.5 \times 10^{12}$ cm^{-3} for the hydrogen, deuterium, and helium plasmas that are explored. The measured vacuum $\imath$ profile is relatively flat, ranging from $\imath(0) = 1.05$ on axis to $\imath = 1.11$ at the plasma edge, with uncertainty in the range of 1%–3%. Quasihelical symmetry in HSX can be degraded by increasing the nonsymmetric magnetic ripple with the introduction of a toroidal mirror term to the magnetic field spectrum using an auxiliary coil set. The nonsymmetric ripple is in addition to the symmetric main helical field ripple which linearly increases from near 0 at the magnetic axis to 12% at the edge. Plasma formation and heating are achieved using second-harmonic X-mode ECRH at 28 GHz with $P_{ECRH} \sim$ 50–150 kW. A consequence of this heating scheme is the generation of fast electrons with high perpendicular velocities ($T_{e\perp} \gg T_{e\parallel}$) as evidenced by electron cyclotron emission, x-ray, and stored energy measurements [14]. Typical bulk electron temperatures are $T_e < 1$ keV while the plasma ions are cold ($T_i \sim 20$ eV). For QHS plasmas at $\bar{n}_e = 1.5 \times 10^{12}$ cm^{-3}, the nonthermal electron tail population is ~4% with temperature ~4.8 keV. At $\bar{n}_e = 0.5 \times 10^{12}$ cm^{-3}, tail population is ~30% at ~12 keV [14].

Temporal evolution of a typical QHS discharge is shown in Fig. 1, where 100 kW of ECRH power terminates at ~30 ms. During the ECRH pulse, a single coherent mode is observed at frequency ~50 kHz on the electron density time trace as measured by interferometry [15]. After ECRH turn-off, the mode decays on a time scale

($\sim$0.2 ms) much faster than the energy confinement time ($\sim$1 ms) as estimated from the stored energy. Evidence for the mode is also observed on external magnetic coils as shown in Fig. 2(a) for a QHS plasma with $\bar{n}_e \approx 0.8 \times 10^{12}$ cm^{-3} and $P_{ECRH} = 50$ kW. For this low density plasma, in addition to the mode at $\sim$50 kHz, another mode at $\sim$72 kHz is also detected. Appearance of the higher-frequency mode is often intermittent, being sensitive to both plasma density (observed primarily at lower densities, $\bar{n}_e \leq 0.8 \times 10^{12}$ cm^{-3}) and heating power. On limited occasions, a third spectral component is also observed at a higher frequency with the same spacing of $\sim$22 kHz. Similar spectral features are measured by interferometer chords with $R - R_0 \leq 4$ cm. Examination of mode phase across chords with varying position reveals that the perturbation has an odd poloidal mode number as a π-phase change is clearly seen for chords on opposite sides of the magnetic axis [see Fig. 2(b)]. Poloidally offset Langmuir probes show that the coherent mode propagates in the diamagnetic drift direction of the bulk electrons, corresponding to $m \geq 1$ in the laboratory frame of reference. In addition, toroidally displaced magnetic and Langmuir probes indicate that the mode has an $n = 1$ toroidal structure where $n > 0$ corresponds to propagation along B_ϕ. The wave at 72 kHz does not appear to be a nonlinearly driven harmonic as n remains unchanged with m being odd. Toroidal propagation along B_ϕ and poloidal propagation in the electron diamagnetic direction leads to $k_\parallel = (n - m\iota)/R < 0$, matching the electron precessional drift direction. However, it is unclear whether passing or trapped particles are responsible for the instability. The mode is not observed for HSX operation with $B = 1$ T, where fundamental O-mode heating at 28 GHz is employed. With this heating configuration, the energetic particle population is significantly reduced as evidenced by a large reduction in the x-ray flux, thereby removing the drive for the instability.
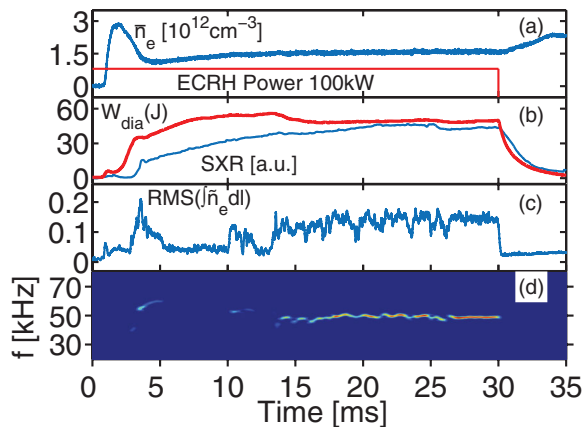
Information on the spatial distribution of the density fluctuations comes from the interferometer data. As shown in Fig. 2(c), the 50 kHz mode has a relative minimum for the chord nearest the magnetic axis as expected for an odd-m perturbation, and the amplitude peaks off-axis near midradius, where the density gradient is steepest. The higher-frequency mode typically peaks at slightly larger radius. Maximum mode amplitude is $\int \tilde{n} dl \approx 3.5 \times 10^{11}$ cm^{-2} with magnetic perturbation $\tilde{B}_\theta/B \approx 4 \times 10^{-5}$ at the wall. Mode activity is observed at all densities up to $\bar{n}_e \leq 2.3 \times 10^{12}$ cm^{-3} on HSX. Measurements show this mode can be continuous or bursting, and in some cases can have small frequency chirps. Mode amplitude is observed to increase with heating power (tripling from 40 to 100 kW) and is not always benign. When the ECRH heating power is at or above 100 kW, the stored energy is degraded by up to 15% with appearance of the mode, beginning at $\sim$14 msec, as shown in Fig. 1(b).

In earlier work on the WVII-AS stellarator [6], a low shear device like HSX, a fast ion driven instability was observed and identified as a global Alfvén eigenmode. Since the mode frequencies observed in HSX are near or below the lowest ($m = 1$, $n = 1$) Alfvén continuum, we also consider global Alfvén eigenmodes as a potential candidate. Fluctuations in the frequency range of 20–120 kHz are observed, and scaling with ion mass density matches reasonably well with the expected $(m_i n_i)^{-1/2}$ scaling for Alfvénic modes [$V_A = B/(4\pi n_i m_i)^{1/2}$]. However, this scaling is inconclusive as the plasma temperature also changes with density and can mask the true features of the mode. Since ECRH is the only source for plasma production and heating, varying the toroidal field (to determine B_T scaling) is not feasible as the resonance location moves. For a purely shear driven Alfvén mode
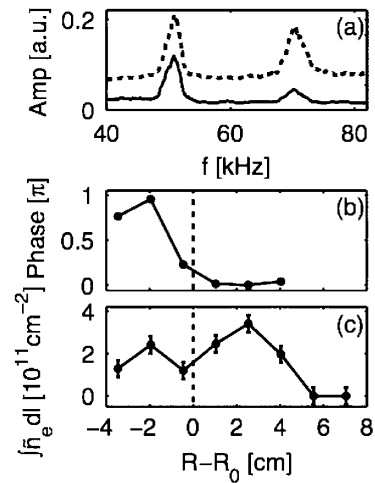

FIG. 1 (color). QHS plasma time series traces for (a) line-averaged electron density ($R - R_0 = -0.5$ cm) and P_{ECRH}, (b) stored energy (W_{dia}) and soft-x-ray (SXR) emission ($r/a = 0.3$), (c) line-integrated fluctuation rms amplitude ($\times 10^{13}$ cm^{-2}), and (d) density fluctuation frequency spectra ($R - R_0 = 2.5$ cm).

FIG. 2. (a) Density (solid line) and dB_θ/dt (dashed line) fluctuation spectra. For the primary mode at $\sim$50 kHz, line-integrated interferometer perturbation (b) phase, and (c) amplitude.

($\omega = k_\parallel V_A$) with $(m, n) = (1, 1)$, the mode frequency is expected to display strong dependence on inverse safety factor through the parallel wave number. In contrast, experimental observations of the mode frequency over the range $0.98 < \iota(0) < 1.12$ exhibit very weak dependence as shown in Fig. 3. For $m = 3$ or larger (and $n = 1$), $k_\parallel$ is much greater than for $(m, n) = (1, 1)$, and the dependence of mode frequency on ι would be strongly diminished. However, for these poloidal mode numbers the Alfvén frequency would rise to >2 MHz making a global Alfvén eigenmode highly unlikely.

To resolve this dilemma, we have included parallel compressibility or finite temperature effects [16] in the mode analysis by considering the shear Alfvén, acoustic, geodesic acoustic, and coupled acoustic–shear Alfvén modes. Acoustic modes are appealing since sound waves have a much larger $k_\parallel$ than Alfvénic modes for a given frequency ($V_A/c_s \approx 100$, where c_s is the sound speed), thereby making them insensitive to changes in inverse safety factor. This treatment is accomplished using the STELLGAP code [17], which has been generalized to solve the coupled set of equations that include Alfvénic modes, sound waves, and their coupling. STELLGAP is a fully toroidal code, using the HSX quasihelically symmetric equilibria and measured profiles, which calculates all eigenvalues of the coupled equations on each flux surface and takes into account interactions between multiple toroidal modes while retaining an adequately resolved Fourier spectrum for the equilibrium quantities.

STELLGAP computed continuum plots for the $n = 0$ and 1 mode families are shown in Fig. 4, where modes with $m = 0$ to 10 for each n have been used. Because of the lack of axial symmetry in stellarators, consideration of single toroidal mode numbers (as in tokamaks) is not adequate, and families of coupled toroidal harmonics must be taken into account. In the case of HSX (4 field periods), the $n = 0$ and 1 mode families include harmonics with $n = \ldots, -5, -4, -3, -1, 0, 1, 3, 4, 5, \ldots$. Roots found at frequencies <5 kHz correspond to $n = 0$ modes which are geodesic acoustic modes that were introduced in
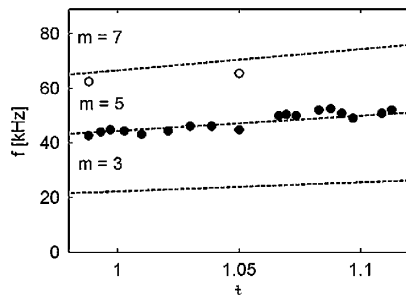
[18] and are thought to play an important role in the development of zonal flows. Bands of higher-frequency acoustic modes that include the $(m, n) = (3, 1)$, $(5, 1)$, and $(7, 1)$ modes are also depicted in Fig. 4. Strong couplings can occur between shear Alfvén and sound continua when their frequencies are similar. A narrow gap, whose position and frequency are sensitive to ι (see Fig. 4), opens in the lowest shear Alfvén continuum ($m = 1$, $n = 1$) that results from including sound wave coupling. Over the broad plasma region where the mode amplitude peaks ($r/a \sim 0.5$), sound waves with $n = 1$, $m = 3$, 5, and 7 represent a reasonably good match to the measured mode frequencies. Likewise, the weak frequency dependence of the mode on ι is well matched by the acoustic mode. For $0.98 < \iota(0) < 1.12$, as shown in Fig. 3, the measured 20% frequency increase is consistent with m in the range 3–7. In addition, separation of frequency bands with odd-m provides a reasonable match to the measured 22 kHz separation between the excited modes. Changes in the mode frequency with temperature (observed by varying the heating power while holding other parameters constant) and ion mass (H, D, He) are consistent with those expected for sound waves.

Insensitivity to ι variation provides evidence that coupling between acoustic modes and Alfvénic modes is weak, implying magnetic perturbations at the acoustic frequency can be viewed as forced perturbations associated with such coupling rather than as evidence of Alfvén eigenmode excitation. It is noteworthy that the coupling links together different poloidal harmonics of the perturbation. This enables magnetic fluctuations to have different mode numbers than density perturbations, as indicated from STELLGAP. Frequency mismatches between computation and experiment can likely be accounted for by a small intrinsic radial electric field, which is unknown, or spatial
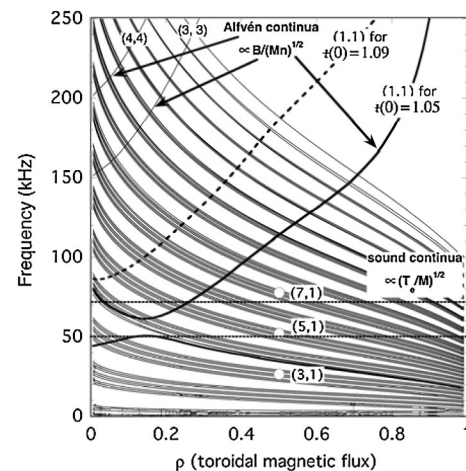
FIG. 3. Mode frequency scaling with inverse safety factor, $\iota(0)$. Measured mode frequencies denoted by solid circles (primary mode) and open circles (secondary mode). Calculated sound wave frequencies for modes with $n = 1$ and $m = 3$, 5, and 7 are shown as dashed lines.

FIG. 4. Coupled Alfvén–sound continua for $n = 0$ and 1 mode families in HSX where $\iota(0) = 1.05$. Open circles at $\rho = (\langle r \rangle/\langle a \rangle)^2 \approx 0.5$ denote sound wave bands containing the (3,1), (5,1), and (7,1) acoustic modes. The observed frequencies of 50 and 72 kHz are marked by horizontal dashed lines. Alfvén (1,1) continuum for $\iota(0) = 1.09$ is shown by a bold dashed tra.
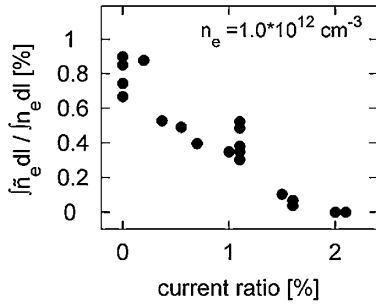
FIG. 5. Mode amplitude dependence on toroidal magnetic perturbation ($P_{ECRH} = 50$ kW). The current ratio represents the strength of the toroidal mirror term (0% denotes QHS configuration).

separation of the modes. Since the variation in the acoustic mode frequency with radius is significantly smaller than that for the Alfvénic mode, global structures are more likely to exist for the former due to reduced phase mixing. Furthermore, ions are cold in HSX ($T_e/T_i > 30$), making ion Landau damping of the acoustic modes exponentially small.

A distinguishing feature of these fluctuations is that they are strongest for quasihelically symmetric HSX plasmas. The measured mode amplitude is found to be extremely sensitive to nonsymmetric magnetic ripple and rapidly decreases with its introduction as shown in Fig. 5. Only a 2% modification [$(\Delta B/B) \approx 2\%$] of the main coil ampere-turns in the auxiliary coils is required to suppress the mode. For this small amplitude perturbation, the energetic particle population appears unchanged as evidenced by the x-ray flux. In addition, the STELLGAP code predicts little change in the continua plots of Fig. 4 when introducing a mirror term of this amplitude.

We conjecture that the reason for the observed dramatic difference in mode excitation between QHS and nonsymmetric stellarator plasmas is the effect of magnetic ripple on the resonant interaction between hot anisotropic electrons and the excited mode. In an idealized case of uniform magnetic field, the resonance condition requires the electron velocity along the magnetic field $V_\parallel$ to be equal to the wave phase velocity $V_{Phase} = \omega/k_\parallel$. As the phase velocity is much smaller than the characteristic value of $V_\perp$ (the electron gyrovelocity), even a slight variation of the magnetic field strength ΔB along the field line can change the electron parallel velocity significantly due to the ∇B force. The corresponding variation in $V_\parallel$ can be estimated as $\delta V_\parallel \approx V_\perp \sqrt{\Delta B/B}$. For acoustic modes, magnetic ripple should affect the resonance condition if $\Delta B/B > (c_s/V_\perp)^2$. The effect of ripple on the Alfvénic resonance should be much weaker, by factor $(V_A/c_s)^2 \approx 1/\beta \sim 10^3$. Although this argument demonstrates very different sensitivities to ripple for the acoustic and Alfvénic resonances, it is still too simplistic, because the magnetic field strength in HSX is not exactly constant along the off-axis field lines due to ripple in the main helical field (symmetric ripple).

However, it is conceivable that the helical symmetry of the inherent magnetic ripple will only shift the resonance to a nearby location in the electron phase space, whereas the symmetry-breaking ripple can break the wave-particle synchronism at the shifted resonance. With these caveats, we note that the extremely high sensitivity of the acoustic resonance to ripple is suggestively consistent with the experimental observations. These considerations call for proper modeling of the resonant particle orbits in the presence of ripple, which we view as an interesting topic for future work.

In summary, a fast-electron-driven instability has been observed in the HSX device. The measured mode frequencies are in the range expected for shear Alfvén and sound waves, while mode propagation is in the electron diamagnetic drift direction. The very weak dependence of the mode frequency on inverse safety factor ι distinguishes the observed mode from shear Alfvénic perturbations. Acoustic modes are the favored global modes in the shear Alfvén–sound wave spectrum of low shear devices like HSX, as they are weakly damped and therefore susceptible to energetic particle destabilization. Mode amplitude sensitivity to magnetic ripple also supports the likelihood of observed instability being a sound wave.

[1] E. D. Fredrickson *et al.*, Phys. Rev. Lett. **87**, 145001 (2001).
[2] S. E. Sharapov *et al.*, Phys. Rev. Lett. **93**, 165001 (2004).
[3] R. Nazikian *et al.*, Phys. Rev. Lett. **91**, 125003 (2003).
[4] M. A. Van Zeeland *et al.*, Plasma Phys. Controlled Fusion **47**, L31 (2005).
[5] K. L. Wong, Plasma Phys. Controlled Fusion **41**, R1 (1999).
[6] A. Weller *et al.*, Phys. Rev. Lett. **72**, 1220 (1994).
[7] M. Takechi *et al.*, Phys. Rev. Lett. **83**, 312 (1999).
[8] S. Yamamoto *et al.*, Phys. Rev. Lett. **91**, 245001 (2003).
[9] G. Y. Fu and J. W. Van Dam, Phys. Fluids B **1**, 1949 (1989).
[10] M. Wakatani, *Stellarator and Heliotron Devices* (Oxford University Press, Oxford, 1998), p. 286.
[11] R. B. White, *The Theory of Toroidally Confined Plasmas* (Imperial College Press, London, 2001).
[12] F. S. B. Anderson *et al.*, Fusion Technol. **27**, 273 (1995).
[13] J. Nuhrenberg and R. Zille, Phys. Lett. A **129**, 113 (1988).
[14] K. M. Likin *et al.*, Plasma Phys. Controlled Fusion **45**, A133 (2003).
[15] C. Deng *et al.*, Rev. Sci. Instrum. **74**, 1625 (2003).
[16] B. N. Breizman *et al.*, Phys. Plasmas **12**, 112 506 (2005).
[17] D. Spong, R. Sanchez, and A. Weller, Phys. Plasmas **10**, 3217 (2003).
[18] N. Winsor, J. L. Johnson, and J. M. Dawson, Phys. Fluids **11**, 2448 (1968).